Letter

Scaling of entropy production under coarse graining in active disordered media

Luca Cocconi,[1,2,3] Guillaume Salbreux,[2] and Gunnar Pruessner[1]
[1]*Department of Mathematics, Imperial College, SW7 2BX London, United Kingdom*
[2]*Department of Genetics and Evolution, University of Geneva, Geneva, Switzerland*
[3]*The Francis Crick Institute, NW1 1AT London, United Kingdom*

(Received 14 September 2021; revised 15 December 2021; accepted 11 March 2022; published 25 April 2022)

Entropy production plays a fundamental role in the study of nonequilibrium systems by offering a quantitative handle on the degree of time-reversal symmetry breaking. It depends crucially on the degree of freedom considered as well as on the scale of description. How the entropy production at one resolution of the degrees of freedom is related to the entropy production at another resolution is a fundamental question which has recently attracted interest. This relationship is of particular relevance to coarse-grained and continuum descriptions of a given phenomenon. In this work, we derive the scaling of the entropy production under iterative coarse graining on the basis of the correlations of the underlying microscopic transition rates for noninteracting particles in active disordered media. Our approach unveils a natural criterion to distinguish equilibrium-like and genuinely nonequilibrium macroscopic phenomena based on the sign of the scaling exponent of the entropy production per mesostate.

DOI: 10.1103/PhysRevE.105.L042601

Introduction. Under the umbrella term of "active matter," the study of systems driven by injection and dissipation of energy at the single-agent level has played a prominent role in the development of nonequilibrium physics and expanded its interface with biology. One of the key challenges that arise when developing models of biological matter is to quantify their degree of "nonequilibriumness," i.e., the extent to which their phenomenology differs from that of a collection of passive particles driven by a bath. The rate of entropy production [1,2] allows for such differentiation by capturing time-reversal symmetry breaking at the microscopic scale [3]. While the injection of energy ensures a strong departure from equilibrium at the single-agent level, these systems do not necessarily exhibit nonequilibrium features at larger spatiotemporal scales [4–8]. The question of whether equilibrium is effectively restored at this mesoscopic level requires new methods to quantify how entropy production varies under spatial coarse-graining [9–15]. We offer a novel perspective on this issue by studying a single-particle driven-diffusion process obtained by perturbing homogeneous diffusion with a nonconservative quenched random forcing. A similar model was recently studied as an effective description for the collective motion of active matter in a random potential [16] and can be seen as a minimal description of a molecular motor self-propelling on a disordered network of cytoskeletal filaments [17]. These models are particular examples of active disordered media [18–21], which we discuss for the first time from a thermodynamic perspective. On a more abstract level, our model may be seen as a many-particle system randomly exploring a complex phase space. From this perspective, our work determines the scaling behavior of entropy production in a wider class of systems, including biochemical reaction networks [15].

We first analyze our model on a one-dimensional ring, where it is exactly solvable [22], and we identify a trivial scaling behavior of the mesoscopic entropy production under block coarse-graining. We then move to higher dimensional lattices, where we show how the mesoscopic entropy production decays algebraically with block size under block coarse-graining. To characterize the nontrivial scaling exponents, we draw on a novel field theoretic formalism based on the Martin-Siggia-Rose construction [23,24] and demonstrate that the scaling of the entropy production can be related to the small wave number behavior of the probability current's spectral density by arguments reminiscent of those employed in the treatment of hyperuniform fluctuations [25]. Our main result, Eq. (18), provides a natural criterion to distinguish between equilibrium-like and genuinely nonequilibrium macroscopic phenomena based on the sign of the scaling exponent for the entropy production per mesostate.

Entropy production and coarse graining. The starting point of our analysis is a Markovian jump process satisfying the master equation

$$\dot{P}_n(t) = \sum_m (P_m(t) w_{m,n} - P_n(t) w_{n,m}) \tag{1}$$

for the probability $P_n(t)$, with $w_{n,m}$ the nonnegative transition rate from state n to state $m \neq n$. The average rate of internal entropy production at steady-state is defined as [2]

$$\dot{S}_i = \frac{1}{2} \sum_{n,m} J_{n,m} \ln \frac{\pi_n w_{n,m}}{\pi_m w_{m,n}}, \tag{2}$$

where $\pi_n = \lim_{t\to\infty} P_n(t)$ is the steady-state probability mass function and $J_{n,m} = \pi_n w_{n,m} - \pi_m w_{m,n}$ is the net probability current from state n to state m. The entropy production $\dot{S}_i$

is nonnegative and vanishes for systems that satisfy detailed balance. Computing $\dot{S}_i$ from Eq. (2) requires complete knowledge of the set of microscopic probability currents $j_{nm} = \pi_n w_{n,m}$, which renders this observable sensitive to time-reversal symmetry breaking induced by energy injection at the microscopic scale. However, this 'fully resolved' entropy production might be of little interest in the discussion of effective descriptions at the mesoscopic scale. In recent years, various works have addressed the issue of coarse-graining, which amounts to a partial loss of information about the microscopic currents j_{nm} [8–10,13,26–28]. The perennial difficulty is that the resulting mesoscopic description is in general non-Markovian [29–31]. Esposito [9] has identified a decomposition of the full entropy production under phase-space partitioning into three nonnegative contributions. Assuming a separation of timescales between intramesostate and intermesostate transitions, it was also shown that the mathematical form of the entropy production, Eq. (2), is recovered at the mesoscopic level.

Previous work has focused on a single coarse-graining step, partly due to constraints of Markovianity. However, if the state space is sufficiently large, then it is natural to ask whether such coarse-graining procedure could be performed iteratively, in a spirit similar to Kadanoff's "block spin" renormalisation [32]. Characterizing the scale dependence of suitable observables such as the entropy production per mesostate,

$$\dot{s}_i^{(\mathrm{meso})} = \dot{S}_i^{(\mathrm{meso})}/N^{(\mathrm{meso})}, \tag{3}$$

with $N^{(\mathrm{meso})}$ the number of mesostates at a given coarse-graining level, will then convey important information regarding the degree of activity at different scales. To carry out this program we first denote the steady-state probability current from mesostate α to mesostate β by

$$j_{\alpha\beta}(L) = \sum_{n\in\alpha}\sum_{m\in\beta} \pi_n w_{n,m}, \tag{4}$$

with L the characteristic coarse-graining length scale, such that $j_{\alpha\beta}(1) = \pi_n w_{nm}$ for $\alpha = \{n\}$ and $\beta = \{m\}$. We then sidestep the issue of Markovianity by postulating an effective mesoscopic entropy production of the form

$$\dot{S}_i^{(\mathrm{meso})}(L) = \frac{1}{2}\sum_{\alpha,\beta}[j_{\alpha\beta}(L) - j_{\beta\alpha}(L)] \ln \frac{j_{\alpha\beta}(L)}{j_{\beta\alpha}(L)}, \tag{5}$$

as would be measured by any observer faithfully applying Eq. (2) to a process observed at a given resolution L. The observable $\dot{S}_i^{(\mathrm{meso})}(L)$ should be thought of as the entropy production of a different (Markovian) process constrained to displaying the coarse-grained currents of the original process. A similar approach has been recently discussed to characterize the scaling of energy dissipation in nonequilibrium reaction networks [15,33].

The model. We will now introduce a minimal driven-diffusion model [34] on a regular lattice, such that the corresponding nonequilibrium steady-state is amenable to iterative block coarse-graining. Diffusion in a stable potential is the prototypical equilibrium phenomenon but there are many ways to modify the familiar diffusive dynamics into a nonequilibrium process, for example by allowing for an unstable potential [35]. An alternative modification, which guarantees a steady state, is to impose periodic boundary conditions in such a way that a global potential function cannot be defined. To see how this is done, we recall [36] that for a Markov jump process, Eq. (1), to have an equilibrium steady state, the affinity

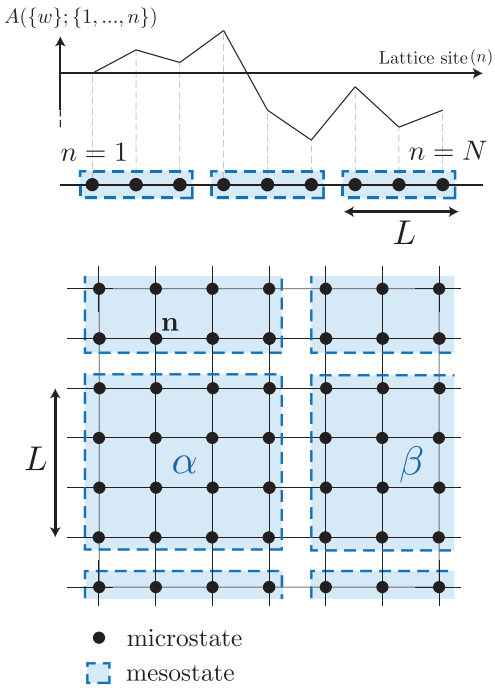

FIG. 1. Coarse-graining procedure for a diffusion process on a periodic square lattice perturbed by a spatially quenched, nonconservative disorder. In one dimension (top), the transition rates locally define a random walk with increments $\nu_n = \zeta_{n,n+1} - \zeta_{n+1,n}$ and the affinity $A(\{w\};\{1,..,N\})$ of the closed cycle across all sites is to leading order proportional to the displacement of the random walk after N steps, Supplemental Material (Sec. I) [39]. In higher dimensions (bottom), the random potential picture breaks down locally and the coarse-graining becomes nontrivial due to the current no longer being uniform.

$$A(\{w\}; n_1, \ldots, n_M) = \ln \frac{w_{n_1,n_2} w_{n_2,n_3} \ldots w_{n_M,n_1}}{w_{n_1,n_M} \ldots w_{n_3,n_2} w_{n_2,n_1}}. \tag{6}$$

of every cycle $\{n_1, n_2, ..., n_M, n_1\}$ has to be exactly zero. Henceforth, we will use the convention that $\ln(0/0) = 0$ as some of the $w_{n,m}$ may vanish. Whenever $A \neq 0$ for any cycle, the system is intrinsically out of equilibrium and we should expect steady-state probability currents [35]. A straightforward way of inducing nonequilibrium behavior is therefore to allow for quenched disorder in the transition rates, which can be interpreted as a nonconservative random forcing [37,38]. The resulting disordered steady-state is then nonequilibrium with exceedingly high probability. In the following we therefore consider a homogeneous diffusion process on a periodic lattice in d dimensions and allow for a quenched perturbation to the nearest-neighbour hopping rates such that

$$w_{n,m} = h + \zeta_{n,m}, \tag{7}$$

with $\zeta_{n,m} > -h$ a set of zero-mean random variables, Fig. 1. Henceforth, $\langle\cdot\rangle$ will denote averages over this random variable.

Ring topology ($d = 1$). The one-dimensional version of this model has previously been considered in the context of random walks in random environments [37,38]. Starting from an exact result by Derrida [22] for the net current, $J = J_{n,n+1}$, the entropy production, Eq. (2), can be calculated as $\dot{S}_i = JA(\{w\}; \{1, 2, \ldots, N\})$, on the basis of constant $J = \pi_n w_{n,n+1} - \pi_{n+1} w_{n+1,n}$ and the affinity A, Eq. (6), taken for the cycle passing through all sites of the ring once [36], Supplemental Material (Sec. I) [39]. After substituting Eq. (7) into Eqs. (6), we eventually obtain

$$\dot{S}_i = \frac{1}{hN^2}\left[\sum_{n=1}^{N}(\zeta_{n,n+1} - \zeta_{n+1,n})\right]^2 + \mathcal{O}(\zeta^3), \tag{8}$$

where $\mathcal{O}(\zeta^k)$ stands for any term proportional to $\zeta_{i_1\pm1,i_1}\ldots\zeta_{i_k\pm1,i_k}$ with any indices $i_1, \ldots, i_k$. As can be seen by setting $\zeta_{i,j} = 0$ for all i, j, the entropy production vanishes at zeroth order in the perturbation, as expected. The Supplemental Material (Sec. I) [39] explores the weak disorder limit of Eq. (8) in more detail [39].

We now apply the coarse-graining procedure based on Eqs. (4) and (5). In one dimension, the interface between distinct mesostates consists of a single edge (Fig. 1) and the net current $j_{\alpha\beta}(L) - j_{\beta\alpha}(L) = J$ is independent of the block size L. The mesoscopic entropy production $\dot{S}_i^{(\mathrm{meso})}$, Eq. (5), is thus given by a sum over a subset of the contributions to the microscopic entropy production $\dot{S}_i$, Eq. (2). By invoking translational invariance and linearity of expectation, the total entropy production rate in a system with originally N states coarse grained into mesostate blocks of size L is

$$\langle\dot{S}_i^{(\mathrm{meso})}\rangle(L) = \left\langle J\sum_{k=1}^{N/L}\ln\frac{\pi_{kL}w_{kL,kL+1}}{\pi_{kL+1}w_{kL+1,kL}}\right\rangle \tag{9}$$

$$= \frac{N}{L}\left\langle J\ln\frac{\pi_n w_{n,n+1}}{\pi_{n+1}w_{n+1,n}}\right\rangle, \tag{10}$$

with arbitrary state index n. For uncorrelated noise in the weak disorder limit and using $\pi_n/\pi_m = r_n/r_m$ [22], $\langle\dot{S}_i^{(\mathrm{meso})}\rangle = 2\lambda/(NhL) + \mathcal{O}(\lambda^2)$, where λ denotes the variance of $\zeta_{n,m}$. Irrespective of the noise strength, the dependence of the total entropy production on the block size L is solely due to the absence of terms from currents within a microstate block. In one dimension, the entropy production per mesostate $\langle\dot{s}_i^{(\mathrm{meso})}\rangle = (L/N)\langle\dot{S}_i^{(\mathrm{meso})}\rangle$, Eq. (3), is thus independent of L. No current averaging at interfaces between blocks takes place. The situation is qualitatively different in $d > 1$, as we will demonstrate now.

Periodic lattices with $d > 1$. In higher dimensions, the equilibrium condition $A(\{w\}; \{n_1, \ldots, n_M\}) = 0$ is generally broken at the local rather than global scale. No analytical expression for the steady-state currents is available and we resort to a perturbation theory in weak disorder, based on a Martin-Siggia-Rose field theory [23,24], which allows us to extract various static correlation functions in arbitrary dimensions and for a wide class of disorders, see Supplemental Material (Sec. II) [39]. There, we introduce the net microscopic probability current $\boldsymbol{J}(\boldsymbol{x}) = [J^{(1)}(\boldsymbol{x}), \ldots, J^{(d)}(\boldsymbol{x})]$ as the continuum limit of $J_{\boldsymbol{n},\boldsymbol{m}}$ on a hypercubic lattice, together with its Fourier transform $\boldsymbol{\mathcal{J}}(\boldsymbol{k}) = (\mathcal{J}^{(1)}(\boldsymbol{k}), \ldots, \mathcal{J}^{(d)}(\boldsymbol{k}))$. We follow the convention

$$J^{(a)}(\boldsymbol{x}) = \frac{1}{V}\sum_{\boldsymbol{k}}\mathcal{J}^{(a)}(\boldsymbol{k})e^{i\boldsymbol{k}\cdot\boldsymbol{x}}, \tag{11}$$

with $\boldsymbol{k} = 2\pi\boldsymbol{n}/(N\ell)$ ($\boldsymbol{n} \in \mathbb{Z}^d$), assuming a hypercubic system, and $V = (N\ell)^d$ the phase space volume, with ℓ the dimensionful lattice spacing. We assume a disorder characterized by the covariance in Fourier space

$$\langle\zeta^{(a)}(\boldsymbol{k})\zeta^{(b)}(\boldsymbol{k}')\rangle = \tilde{\lambda}|\boldsymbol{k}|^{-\eta}\delta_{ab}V\delta_{\boldsymbol{k}+\boldsymbol{k}',0} \tag{12}$$

for $|\boldsymbol{k}| \to 0$, corresponding, for $\eta \neq 0$, to $\langle\zeta^{(a)}(\boldsymbol{r})\zeta^{(b)}(\boldsymbol{r}')\rangle \sim \delta_{ab}|\boldsymbol{r} - \boldsymbol{r}'|^{-d+\eta}$ at $|\boldsymbol{r} - \boldsymbol{r}'| \to \infty$, where $\zeta^{(a)}$ indicates the disorder affecting edges parallel to the a-th dimension of the lattice (see Supplemental Material (Sec. II) [39] for details of the specification of backward rates). The spectral density tensor of the probability current evaluated at tree level then reads (Supplemental Material (Sec. II) [39]), for $\boldsymbol{k} \neq 0$,

$$\langle\mathcal{J}^{(a)}(\boldsymbol{k})\mathcal{J}^{(b)}(\boldsymbol{k}')\rangle = \frac{4\tilde{\lambda}}{V}\left(\delta_{ab} - \frac{k_a k_b}{|\boldsymbol{k}|^2}\right)|\boldsymbol{k}|^{-\eta}\delta_{\boldsymbol{k}+\boldsymbol{k}',0}. \tag{13}$$

Equation (13) matches the general form of the spectral density of a divergence-free, isotropic vector field, which is well known from the theory of turbulence of incompressible fluids [40,41]. For $\eta < 0$, the vanishing of the spectral density as $\boldsymbol{k} \to 0$ indicates that the probability current is hyperuniform [25], i.e., exhibits an anomalous suppression of fluctuations at large wavelengths. The case $\eta = 0$ corresponds to uncorrelated (white) noise, $\langle\zeta^{(a)}(\boldsymbol{r})\zeta^{(b)}(\boldsymbol{r}')\rangle = \tilde{\lambda}\delta_{ab}\delta(\boldsymbol{r} - \boldsymbol{r}')$.

We can now carry out the coarse-graining procedure for the entropy production. First, we note that the mesoscopic entropy production, Eq. (5), is given by a sum over contributions from neighboring mesostates, $\alpha \neq \beta$ in Eq. (5). By linearity of expectation, the disorder average $\langle\dot{S}_i^{(\mathrm{meso})}\rangle$ is therefore the expected contribution from a single interface multiplied by the number of interfaces. It follows that, for a hypercubic lattice with coordination number $2d$,

$$\langle\dot{s}_i^{(\mathrm{meso})}\rangle = d\left\langle[j_{\alpha\beta}(L) - j_{\beta\alpha}(L)]\ln\frac{j_{\alpha\beta}(L)}{j_{\beta\alpha}(L)}\right\rangle, \tag{14}$$

where $\{\alpha, \beta\}$ is any pair of neighboring mesostates. Asymptotically in large L, Eq. (14) can be approximated by

$$\langle\dot{s}_i^{(\mathrm{meso})}\rangle \simeq \frac{dN^d}{hL^{d-1}}\sigma_J^2(L), \tag{15}$$

where

$$\sigma_J^2(L) = \langle(j_{\alpha\beta}(L) - j_{\beta\alpha}(L))^2\rangle \tag{16}$$

denotes the variance of the probability current integrated across an interface of linear dimension L. This relation is derived in Supplemental Material (Sec. III) [39]. In the continuum limit, the asymptotic scaling of the entropy production per mesostate is therefore controlled by the asymptotic variance of the current integrated across the interface between states, which is in turn determined by the small wave number behavior of the current spectral density tensor introduced in

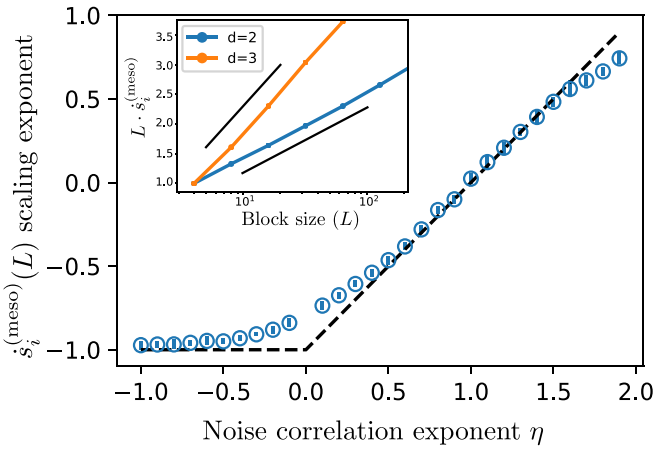

FIG. 2. The dependence of the scaling exponent for the entropy production per mesostate, $\dot{s}_i^{(\mathrm{meso})}$, on η in the range $-1 \leqslant \eta \leqslant d$, shown here for $d = 2$ and $N = 2048^2$, is well captured by Eq. (18), shown in black dashed. For uncorrelated disorder, $\eta = 0$, the algebraic scaling of $\dot{s}_i^{(\mathrm{meso})}$ with block size L displays a logarithmic correction, shown in the inset for $d = 2, 3$, also in agreement with Eq. (18). Exact logarithmic scaling is shown in solid black for reference. The ordinate is here normalised to its value for the smallest block size considered.

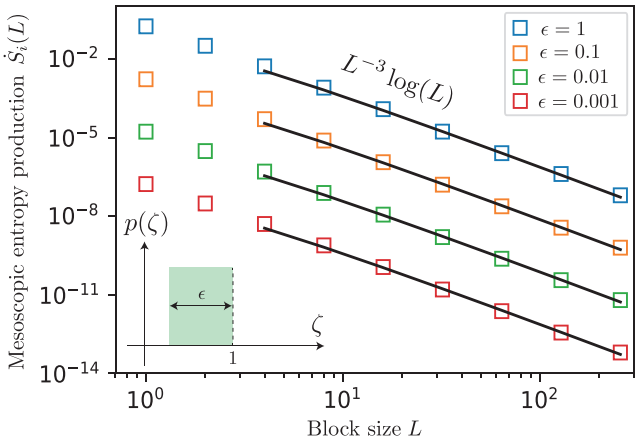

FIG. 3. Mesoscopic entropy production as a function of block size and predicted scaling according to Eq. (18) (case $d = 2$, $\eta = 0$) for various noise strengths. The predicted scaling appears to hold numerically beyond the weak disorder approximation. The noise $\zeta_{n,m}$ is taken from a uniform distribution with support $\zeta \in \{[-1, -(1-\epsilon)) \cup (1-\epsilon, 1]\}$ and $h = 1$ to ensure positivity of the transition rates.

Eq. (13). In fact, the relationship between Eqs. (13) and (16) is exactly the type of problem addressed in the study of hyperuniform systems [25]. Using results from these studies, one obtains

$$\sigma_J^2(L) \sim \begin{cases} L^{d-2}, & \text{for } \eta < 0, \\ L^{d-2}\ln(L), & \text{for } \eta = 0, \\ L^{d-2+\eta}, & \text{for } 0 < \eta < d. \end{cases} \tag{17}$$

A more thorough derivation of these scaling laws is provided in Supplemental Material (Sec. IV) [39]. We can think of $\sigma_J^2(L) \sim L^{d-2}$ as scaling with the perimeter of the interface. In this sense, it is instructive to draw a comparison with the case of a nonsolenoidal random vector field with spectral density $\langle \mathcal{J}^{(a)}(\boldsymbol{k})\mathcal{J}^{(b)}(\boldsymbol{k}')\rangle = (\tilde{\lambda}/V)\delta_{ab}\delta_{\boldsymbol{k}+\boldsymbol{k}',0}$, in which case the variance of the integrated current instead scales with the area of the interface, $\sigma_J^2(L) \sim L^{d-1}$. The requirement that the steady state is divergence-free thus plays an important role by imposing long-range correlations in the currents, even when these are not present in the substrate, i.e., for $\eta = 0$. Combining Eqs. (15) and (17) we eventually arrive at (Supplemental Material (Sec. IV) [39])

$$\langle \dot{s}_i^{(\mathrm{meso})} \rangle(L) \propto \frac{\sigma_J^2(L)}{L^{d-1}} \sim \begin{cases} L^{-1}, & \text{for } \eta < 0, \\ L^{-1}\ln(L), & \text{for } \eta = 0, \\ L^{-1+\eta}, & \text{for } 0 < \eta < d, \end{cases} \tag{18}$$

which constitutes our key result. The scaling exponent changes sign at $\eta = 1$, corresponding to $\langle \zeta^{(a)}(\boldsymbol{r})\zeta^{(b)}(\boldsymbol{r}')\rangle \sim \delta_{ab}|\boldsymbol{r} - \boldsymbol{r}'|^{-(d-1)}$, suggesting a quantitative distinction between steady states that are increasingly "equilibriumlike" at larger scales and genuinely nonequilibrium states where dissipation occurs at all scales. Numerical simulations for $\eta = 0$ in $d = 2, 3$, as well as the full range $-1 < \eta < d$ in $d = 2$ show excellent agreement with our analytical prediction (see Fig. 2).

Investigating entropy production numerically indicates that this scaling behavior of the entropy production is unchanged in the strong disorder regime (Fig. 3).

Concluding remarks and outlook. Based on the effective entropy production introduced in Eq. (5), we have studied the mesoscopic scaling of the entropy production per mesostate under iterative block coarse graining for a family of nonequilibrium disordered steady states with generic substrate correlations. We demonstrate that coarse-graining of degrees of freedom results in nontrivial *scaling* of the entropy production, Eqs. (18), so that its value on one scale is related to its value on another scale in a nontrivial fashion that ultimately draws on the correlations of the transition rates, Eq. (12). To characterize our model we have developed a static field-theoretic framework, which complements recent work [42] by considering problems involving multiplicative noise. Our main result, Eq. (18), offers conditions for which active disordered media appear equilibriumlike, $\eta \leqslant 1$, or genuinely nonequilibrium, $\eta > 1$, at the large scale and in a statistical sense, i.e., when the behavior is averaged over many realisations.

Experiments. A natural application of the theory above of active disordered media are active particles [43] on irregular surfaces, which phenomenologically behave as randomly driven passive particles [16]. This is due to ratchet effects, i.e., local asymmetries in the potential driving a net current [44]. In this case, correlations in the medium can be induced by controlling the ruggedness of the substrate [45]. Further, *in vitro* experiments involving active transport by molecular motors in a network of cytoskeletal filaments [46,47] often involve cell extracts where these filaments are uniformly disordered ($\eta = 0$). Nontrivial, long-range correlations in this type of systems could be induced, e.g., by coupling tagged filaments to an external magnetic field, as done in Ref. [48] with actin.

Acknowledgments. L.C. thanks R. G.-Millan, S. Torquato, N. Antonov, and P. Kakin for fruitful discussion at various stages of this work. L.C. and G.S. acknowledge support from

the Francis Crick Institute, which receives its core funding from Cancer Research UK (Grant No. FC001317), the UK Medical Research Council (Grant No. FC001317), and the Wellcome Trust (Grant No. FC001317).

[1] U. Seifert, Stochastic thermodynamics, fluctuation theorems and molecular machines, Rep. Prog. Phys. 59 (2012).
[2] L. Cocconi, R. Garcia-Millan, Z. Zhen, B. Buturca, and G. Pruessner, Entropy production in exactly solvable systems, Entropy **22**, 1252(2020).
[3] P. Gaspard, Time-Reversed Dynamical Entropy and Irreversibility in Markovian Random Processes, J. Stat. Phys. **117**, 599 (2004).
[4] C. Nardini, É. Fodor, E. Tjhung, F. van Wijland, J. Tailleur, and M. E. Cates, Entropy Production in Field Theories Without Time-Reversal Symmetry: Quantifying the Nonequilibrium Character of Active Matter, Phys. Rev. X **7**, 021007 (2017).
[5] P.-S. Shim, H.-M. Chun, and J. D. Noh, Macroscopic time-reversal symmetry breaking at a nonequilibrium phase transition, Phys. Rev. E **93**, 012113 (2016).
[6] D. A. Egolf, Equilibrium regained: From nonequilibrium chaos to statistical mechanics, Science **287**, 101 (2000).
[7] M. E. Cates and J. Tailleur, Motility-induced phase separation, Annu. Rev. Condens. Matter Phys. **6**, 219 (2015).
[8] S. Dorosz and M. Pleimling, Entropy production in the nonequilibrium steady states of interacting many-body systems, Phys. Rev. E **83**, 031107 (2011).
[9] M. Esposito, Stochastic thermodynamics under coarse graining, Phys. Rev. E **85**, 041125 (2012).
[10] C. P. Amann, T. Schmiedl, and U. Seifert, Communications: Can one identify nonequilibrium in a three-state system by analyzing two-state trajectories? J. Chem. Phys. **132**, 041102 (2010).
[11] A. Gomez-Marin, J. M. R. Parrondo, and C. Van den Broeck, Lower bounds on dissipation upon coarse graining, Phys. Rev. E **78**, 011107 (2008).
[12] J. Li, J. M. Horowitz, T. R. Gingrich, and N. Fakhri, Quantifying dissipation using fluctuating currents, Nat. Commun. **10**, 1 (2019).
[13] F. Caballero and M. E. Cates, Stealth Entropy Production in Active Field Theories Near Ising Critical Points, Phys. Rev. Lett. **124**, 240604 (2020).
[14] A. Celani, S. Bo, R. Eichhorn, and E. Aurell, Anomalous Thermodynamics at the Microscale, Phys. Rev. Lett. **109**, 260603 (2012).
[15] Q. Yu, D. Zhang, and Y. Tu, Inverse Power Law Scaling of Energy Dissipation Rate in Nonequilibrium Reaction Networks, Phys. Rev. Lett. **126**, 080601 (2021).
[16] S. Ro, Y. Kafri, M. Kardar, and J. Tailleur, Disorder-Induced Long-Ranged Correlations in Scalar Active Matter, Phys. Rev. Lett. **126**, 048003 (2021).
[17] A. Kahana, G. Kenan, M. Feingold, M. Elbaum, and R. Granek, Active transport on disordered microtubule networks: The generalized random velocity model, Phys. Rev. E **78**, 051912 (2008).
[18] K. S. Olsen, L. Angheluta, and E. G. Flekkøy, Active Brownian particles moving through disordered landscapes, Soft Matter **17**, 2151 (2021).
[19] F. Peruani and I. S. Aranson, Cold active motion: How Time-Independent Disorder Affects the Motion of Self-Propelled Agents, Phys. Rev. Lett. **120**, 238101 (2018).
[20] O. Chepizhko and F. Peruani, Active particles in heterogeneous media display new physics, Eur. Phys. J.: Spec. Top. **224**, 1287 (2015).
[21] E. Pinçe, S. K. Velu, A. Callegari, P. Elahi, S. Gigan, G. Volpe, and G. Volpe, Disorder-mediated crowd control in an active matter system, Nat. Commun. **7**, 10907 (2016).
[22] B. Derrida, Velocity and diffusion constant of a periodic one-dimensional hopping model, J. Stat. Phys. **31**, 433 (1983).
[23] J. Zinn-Justin, *Quantum Field Theory and Critical Phenomena*, Vol. 171 (Oxford University Press, Oxford, UK, 2021)
[24] J. A. Hertz, Y. Roudi, and P. Sollich, Path integral methods for the dynamics of stochastic and disordered systems, J. Phys. A: Math. Theor. **50**, 033001 (2017).
[25] S. Torquato, Hyperuniformity and its generalizations, Phys. Rev. E **94**, 022122 (2016).
[26] S. Rahav and C. Jarzynski, Fluctuation relations and coarse-graining, J. Stat. Mech.: Theory Exp. (2007) P09012.
[27] A. Gomez-Marin, J. M. R. Parrondo, and C. V. den Broeck, The "footprints" of irreversibility, Europhys. Lett. **82**, 50002 (2008).
[28] G. Nicolis, Transformation properties of entropy production, Phys. Rev. E **83**, 011112 (2011).
[29] P. Strasberg and M. Esposito, Non-Markovianity and negative entropy production rates, Phys. Rev. E **99**, 012120 (2019).
[30] S. Bo and A. Celani, Multiple-scale stochastic processes: Decimation, averaging and beyond, Phys. Rep. **670**, 1 (2017).
[31] G. Teza and A. L. Stella, Exact Coarse Graining Preserves Entropy Production Out of Equilibrium, Phys. Rev. Lett. **125**, 110601 (2020).
[32] L. P. Kadanoff, Scaling laws for Ising models near T_c, Phys. Phys. Fiz. **2**, 263 (1966).
[33] Q. Yu and Y. Tu, State-space renormalization group theory of nonequilibrium reaction networks: Exact solutions for hypercubic lattices in arbitrary dimensions, arXiv preprint arXiv:2201.05746 (2022).
[34] B. Schmittmann and R. K. P. Zia, Statistical mechanics of driven diffusive systems, in *Phase Transitions and Critical Phenomena*, edited by C. Domb and J. L. Lebowitz (Academic Press, New York, NY, 1995), Vol. 17, pp. 1–220
[35] J. Wang, Landscape and flux theory of non-equilibrium dynamical systems with application to biology, Adv. Phys. **64**, 1 (2015).
[36] J. Schnakenberg, Network theory of microscopic and macroscopic behavior of master equation systems, Rev. Mod. Phys. **48**, 571 (1976).
[37] L. V. Bogachev, Random walks in random environments, Encyc. Math. Phys. **4**, 353 (2006).
[38] J.-P. Bouchaud and A. Georges, Anomalous diffusion in disordered media: Statistical mechanisms, models and physical applications, Phys. Rep. **195**, 127 (1990).
[39] See Supplemental Material at http://link.aps.org/supplemental/10.1103/PhysRevE.105.L042601, which includes Refs. [49–53], for additional details of the calculations at the basis of the results presented in the main text.
[40] D. Forster, D. R. Nelson, and M. J. Stephen, Large-distance and long-time properties of a randomly stirred fluid, Phys. Rev. A **16**, 732 (1977).

[41] A. S. Monin and A. Yaglom, *Statistical Fluid Mechanics: Mechanics and Turbulence* (MIT Press, Cambridge, MA, 1975), Vol. 2.

[42] N. V. Antonov, P. I. Kakin, and N. M. Lebedev, Static approach to renormalization group analysis of stochastic models with spatially quenched disorder, J. Stat. Phys. **178**, 392 (2020).

[43] C. Bechinger, R. Di Leonardo, H. Löwen, C. Reichhardt, G. Volpe, and G. Volpe, Active particles in complex and crowded environments, Rev. Mod. Phys. **88**, 045006 (2016).

[44] C. O. Reichhardt and C. Reichhardt, Ratchet effects in active matter systems, Annu. Rev. Condens. Matter Phys. **8**, 51 (2017).

[45] S. Yu, C.-W. Qiu, Y. Chong, S. Torquato, and N. Park, Engineered disorder in photonics, Nat. Rev. Mater. **6**, 226 (2021).

[46] H. Salman, A. Abu-Arish, S. Oliel, A. Loyter, J. Klafter, R. Granek, and M. Elbaum, Nuclear localization signal peptides induce molecular delivery along microtubules, Biophys. J. **89**, 2134 (2005).

[47] Y. Bashirzadeh and A. P. Liu, Encapsulation of the cytoskeleton: Towards mimicking the mechanics of a cell, Soft Matter **15**, 8425 (2019).

[48] Y. Chen, S. Guzik, J. P. Sumner, J. Moreland, and A. P. Koretsky, Magnetic manipulation of actin orientation, polymerization, and gliding on myosin using superparamagnetic iron oxide particles, Nanotechnology **22**, 065101 (2011).

[49] S. R. De Groot and P. Mazur, *Non-Equilibrium Thermodynamics* (Dover Publications, New York, NY, 2003).

[50] A. Compte and J.-P. Bouchaud, Localisation in 1D random random walks, J. Phys. A: Math. Gen. **31**, 6113 (1998).

[51] B. B. Mandelbrot and J. W. V. Ness, Fractional Brownian motions, fractional noises, and applications, SIAM Rev. **10**, 422 (1968).

[52] H. Bateman, *Higher Transcendental Functions* (McGraw-Hill Book Company, New York, NY, 1953), Vol. 1.

[53] J. Kim and S. Torquato, Effect of window shape on the detection of hyperuniformity via the local number variance, J. Stat. Mech.: Theory Exp. (2017) 013402.